Icarus **143**, 159–169 (2000)
doi:10.1006/icar.1999.6236, available online at http://www.idealibrary.com on IDEAL®

Dust around Herbig Ae/Be Stars: Porous, Cometary-Like Grains?

Natalia A. Krivova

Max-Planck-Institut für Aeronomie, D-37191 Katlenburg-Lindau, Germany; and Astronomical Institute, St. Petersburg University, 198904 St. Petersburg, Russia
E-mail: natalie@linmpi.mpg.de

and

Vladimir B. Il'in

Astronomical Institute, St. Petersburg University, 198904 St. Petersburg, Russia

Received September 28, 1998; revised June 7, 1999

Herbig Ae/Be (HAeBe) stars are pre-main sequence objects of moderate mass representing the early evolutionary stages of β Pic-type stars. The objects of both kinds are surrounded by dust disks/shells, and the dust is believed to be continually replenished by comet-like bodies orbiting close to the stars. As the dust particles in the β Pictoris disk are likely to be as fluffy as cometary dust is, it is reasonable to suppose that the grains around HAeBe stars could be porous as well. This brings up the question, which we try to answer here, of how the grain porosity affects the observational manifestations of the dust shells of HAeBe stars: the excess infrared emission, anomalous extinction in the ultraviolet, and the peculiar behavior of color indices and linear polarization during deep brightness minima observed for about 25% of HAeBe stars (UX Ori, WW Vul, etc).

We have performed numerical Monte Carlo simulations of polarized radiation transfer in spheroidal inhomogeneous shells for three different models of circumstellar dust grains. In addition to the observational data mentioned above, intensity scans and polarization maps of the objects have been constructed in view of possible future observations. It is found that the porosity of circumstellar grains weakly affects the spectral energy distribution (when the grain model does not include particles with quite different optical properties) and does not show pronounced effects in the intensity and polarization maps for all grain models considered. On the other hand, the porosity normally reduces single-scattering albedo of particles, and therefore, fluffy grains explain the spectral energy distributions of UX Ori-like stars and their tracks in the color–magnitude diagrams considered in combination much better than compact grains do. However, highly porous, cometary-like grains are unlikely to be abundant in the shells as they produce too low linear polarization to account for the observations of the HAeBe stars. © 2000 Academic Press

Key Words: **radiative transfer; polarimetry; interplanetary dust; comets.**

1. INTRODUCTION

Large infrared excesses detected by the Infrared Astronomical Satellite (IRAS) for Vega and several other main-sequence stars were commonly attributed to the thermal emission of circumstellar dust. The interest in the objects has quickened when recent observations showed the presence of a circumstellar disk around β Pictoris—the best studied object among Vega-type stars—and provided evidence of planet formation in the disk.

The precursors of the Vega-type stars are thought to be Herbig Ae/Be (HAeBe) stars—young intermediate-mass (2–8 $M_\odot$) stars surrounded by dusty shells (or disks). Evidently, the study of the dust shells of these stars along with the disks of Vega-type stars should provide a better understanding of the formation process of planetary systems.

The formation of dust grains in the shells of HAeBe stars is hardly possible, and stellar radiation pressure should quickly blow grains out of the vicinities of the stars. Therefore, some authors believe that the dust particles are continuously delivered to the internal layers of the shells by comet-like bodies (e.g., Voshchinnikov and Grinin 1991, Grinin *et al.* 1996). A similar hypothesis was suggested to explain the presence of dust around β Pic and other Vega-type stars (Harper *et al.* 1984, Weissman 1985, Telesco *et al.* 1988).

In modeling of the dusty shells of HAeBe stars one always used compact particles (e.g., Sorrell 1990, Grinin *et al.* 1991, Voshchinnikov *et al.* 1996, Miroshnichenko *et al.* 1997, Pezzuto *et al.* 1997). There are arguments, however, in favor of their fluffiness. For instance, if there is a strong processing of the grains in the comet-like bodies, the circumstellar particles should resemble cometary grains which are known to be porous. Even if the hypothesis on the comet-like bodies is not correct, the circumstellar particles should be similar to interstellar grains, and these latter are fluffy in accordance with some contemporary interstellar dust models (see, e.g., Henning (1997) and references therein). It can be also noted that fluffiness of the grains in the disk of β Pic allows one to interpret available observational data in a more consistent way (Li and Greenberg 1998). An evidence in favor of a porous structure of the grains in the shells of HAeBe stars may be a possibly low value of albedo of the circumstellar particles (Krivova and Il'in 1997).

0019-1035/00 $35.00

In this paper we consider the effects of grain porosity on the observational appearance of the dust shells: the spectral energy distribution from the infrared to the ultraviolet, the variations of the color indices for the HAeBe stars with Algol-like minima, the wavelength dependence of the linear polarization degree, intensity scans, and polarization maps. The model used is described in Section 2, and the results of our calculations are discussed in Section 3 with conclusions given in Section 4.

2. MODEL

Porous Dust Grains

As the nature of the circumstellar grains is not fully understood, to represent them we use three different models of interstellar dust grains: (1) the model of Li and Greenberg (1997) with very fluffy, cometary-like aggregates of grains, (2) the recent Mathis (1996) model of interstellar dust with inhomogeneous grains of a moderate porosity, and (3) the classical model of Mathis *et al.* (1977; hereafter MRN) with initially compact grains. In all the models the porosity of particles is an additional varying parameter.

The grain model of Li and Greenberg (1997) was selected as a basic one since it is close to the models of cometary dust and dust grains in the β Pic disk suggested by Greenberg and Hage (1990) and Li and Greenberg (1998), respectively. The model implies that submicrometer grains have a silicate core and an organic refractory mantle and form porous aggregates. As is customary, the aggregates are represented by homogeneous spheres with an effective refractive index defined by the Bruggeman rule (see, e.g., Bohren and Huffman (1983) for more details). Such an approach called the Effective Medium Theory (EMT) works well in many cases and gives a reasonable first approximation in some others (Bohren and Huffman 1983, Wolff *et al.* 1994, Stognienko *et al.* 1995).

The EMT is applied to find the effective refractive indices both of the core–mantle subparticles and, then, of their porous aggregates. The volume ratio of the silicate core to the organic refractory mantle is taken equal to one. For aggregates, the filling factor f ($f = 1 - P$, where P is the porosity of aggregates, i.e., the filling factor of vacuum) is varied from 0.1 to 0.01. Only single-size aggregates are considered as the size distribution of dust grains in the shells is quite uncertain. The refractive indices of Li and Greenberg (1997) have been adopted for the materials. The optical properties of the effective homogeneous spheres are calculated using the Mie theory.

In the model of Mathis (1996) interstellar grains of submicrometer size are assumed to be aggregates of silicate and amorphous carbon subparticles. The aggregates have a rather moderate porosity ($f \sim 0.5$) and the size distribution

$$n(a) \propto a^{-q} e^{-(\gamma_1 a + \gamma_2/a + \gamma_3 a^2)}, \qquad (1)$$

where γ_1, γ_2, γ_3 are constants. To treat such fluffy inhomogenous particles we use again the EMT, namely, the Bruggeman rule for three components. The refractive index of amorphous carbon is taken from Rouleau and Martin (1991), and that of silicate—from Laor and Draine (1993). The volume ratio of silicate to amorphous carbon is 0.5 (Mathis 1996), and the filling factor $f = (1 - P)$ is varied from 0.5 to 0.1.

The MRN model well describes the optical properties of interstellar grains and was practically always used in modeling of radiative transfer in circumstellar dust shells. This model involves bare silicate and graphite spherical particles with a power-law size distribution. The model parameters are the exponent of the distribution, the maximum and minimum particle sizes and the ratio (by number) of silicate grains to graphite ones. We included one more parameter—the porosity of the grains P—and varied the material filling factor $f = (1 - P)$ in the wide range from 1 to 0.03. The refractive indices of silicate and graphite are from Laor and Draine (1993), and again the Bruggeman rule is used.

We do not discuss here the advantages and disadvantages of the dust grain models used but refer a reader to the corresponding papers and reviews (e.g., Mathis 1990, 1998; Draine 1994).

Note that some calculations for Mathis (1996) and MRN models have been briefly described in our earlier works (Krivova *et al.* 1998, Il'in and Krivova 2000). In this paper we mainly present the results obtained within the Li and Greenberg (1997) approach and compare them with those derived within two other approaches in order to draw conclusions which would be less "model-dependent."

Shell Geometry

It is assumed that the star is surrounded by an extended dust shell with the density distribution

$$n(\mathbf{r}) = n_0 \left[\sqrt{r_x^2 + r_y^2 + \left(\frac{A}{B}\right)^2 r_z^2} \right]^{-\alpha}, \qquad (2)$$

where $\mathbf{r} = (r_x, r_y, r_z)$ is the radius vector, n_0 and α are some constants, and the surfaces of equal density are oblate spheroids with the aspect ratio A/B. The inclination angle is φ, and the longitude of ascending mode is always 90° for the sake of simplicity.

Because of grain sublimation there must be a dust-free hole of radius $R_{\rm in}$ at the center of the shell. It is difficult to distinguish between the distant, rarefied layers of the shells and interstellar matter and hence to define the outer radius $R_{\rm out}$. Fortunately, reasonable variations of $R_{\rm out}$ only slightly affect the flux from the object in the spectral region being considered.

It should be mentioned that the geometry of the dust shells of HAeBe stars has been the subject of a long discussion—do they form an extended shell or a more compact disk?—and up to now there has been no definite conclusion (see, e.g., Berrilli *et al.* 1992, Pezzuto *et al.* 1997). Perhaps, both geometries exist concurrently.

Radiation of the Objects

The radiation of a star surrounded by a dust shell is the sum of the stellar radiation (flux F_λ^*) partly absorbed and scattered by dust grains in the line of sight, the radiation scattered in the shell in the direction of the observer ($F_\lambda^{\rm sca}$), and the thermal radiation of circumstellar dust particles ($F_\lambda^{\rm therm}$)

$$F_\lambda = F_\lambda^* e^{-\tau_\lambda} + F_\lambda^{\rm sca} + F_\lambda^{\rm therm}, \quad (3)$$

where τ_λ is the optical thickness of the shell along the line of sight (the source is assumed to be unresolved). Note that in our model $F_\lambda^{\rm sca}$ and τ_λ depend on the inclination angle φ.

The spectral energy distribution is usually constructed in the visual and infrared. In the ultraviolet the circumstellar extinction curves are typically considered instead of it. The circumstellar extinction is the ratio of the fluxes of a star with the dust shell and the star without the shell

$$A_\lambda = -2.5 \log\left(\frac{F_\lambda}{F_\lambda^*}\right). \quad (4)$$

Note that the circumstellar extinction differs from that in the line of sight (τ_λ) because of the contribution of scattered radiation.

Brightness Minima

We adopt the hypothesis of Grinin (1988) that the brightness minima are due to screens (clouds, clumps in the shells) appearing in the line of sight between the star and an observer (see discussion in Herbst *et al.* (1994), Zaitseva and Lyutyi (1997)). If the optical thickness of such a clump is $\tau_\lambda^{\rm cl}$, the total flux is

$$F_\lambda\left(\tau_\lambda^{\rm cl}\right) = F_\lambda^* e^{-\tau_\lambda - \tau_\lambda^{\rm cl}} + F_\lambda^{\rm sca} + F_\lambda^{\rm therm}, \quad (5)$$

where we imply that the size of the clump $R^{\rm cl} \ll R^{\rm in}$ considering that Voshchinnikov and Grinin (1991) estimated the clump sizes as a few tenths of astronomic unit.

Then the dependence of the stellar magnitude of the object on the optical thickness of such a screen is

$$\Delta m_\lambda\left(\tau_\lambda^{\rm cl}\right) = -2.5 \log\left[\frac{F_\lambda^* e^{-\tau_\lambda - \tau_\lambda^{\rm cl}} + F_\lambda^{\rm sca} + F_\lambda^{\rm therm}}{F_\lambda^* e^{-\tau_\lambda} + F_\lambda^{\rm sca} + F_\lambda^{\rm therm}}\right], \quad (6)$$

and for a color index

$$\Delta(X - Y) = \Delta m_{\lambda_X} - \Delta m_{\lambda_Y}, \quad (7)$$

where X, Y are the photometric band names, and λ_X, λ_Y are their wavelengths.

We do not consider the optical properties of dust in the clumps as they may strongly differ from those of "diffuse" dust in the shell. Information on grains in the clumps is rather insufficient and at the moment it comes mainly from the slopes of the upper parts of the dependence $\Delta(X - Y)$ on Δm (Friedemann *et al.* 1993). Therefore, we adopt

$$\tau_{\lambda_X}^{\rm cl} = \left(\frac{\lambda_X}{\lambda_V}\right)^{-\beta_{XV}} \tau_{\lambda_V}^{\rm cl}, \quad (8)$$

where the exponents β_{XV} are determined from the observed slopes of the upper parts of the color tracks following Voshchinnikov (1989), and $\tau_V^{\rm cl}$ is a parameter. To simulate the tracks of a star in the color–magnitude diagrams, we vary this parameter from 0 to a very large value ($\tau_V^{\rm max}$). Note that observed brightness drops exceed $1.5–2^m$, which means that $\tau_V^{\rm cl}$ should be large. Then the tracks weakly depend on variations of $\tau_V^{\rm max}$.

Linear Polarization

All three components of radiation of the object (see Eq. (3)) can be polarized: (i) the transmitted radiation if there are aligned nonspherical grains in the line of sight, (ii) the scattered radiation because of nonspherically symmetric density distribution (see, e.g., Grinin 1994), and (iii) the thermal radiation if dust particles in the shell are nonspherical and aligned. It is easy to get the following expression for the total polarization (Krivova 1998)

$$\mathbf{P}_\lambda = \mathbf{P}_\lambda^{\rm cs}\left(1 - \frac{F_\lambda^{\rm sca} + F_\lambda^{\rm therm}}{F_\lambda}\right) + \mathbf{P}_\lambda^{\rm sca}\frac{F_\lambda^{\rm sca}}{F_\lambda} + \mathbf{P}_\lambda^{\rm therm}\frac{F_\lambda^{\rm therm}}{F_\lambda}, \quad (9)$$

where $P_\lambda^{\rm cs}$ is proportional to the difference of the optical thickness τ_λ for light polarized in two perpendicular directions.

We are interested in the polarization only within the visual and near-infrared wavelength regions ($\lambda < 1\,\mu$m), where the ratio $F_\lambda^{\rm therm}/F_\lambda$ is small. When an eclipse of the star occurs, the polarization should change with the object brightness as

$$\mathbf{P}_\lambda(\Delta m_\lambda) \approx \mathbf{P}_\lambda^{\rm cs}\left(1 - \frac{F_\lambda^{\rm sca}}{F_\lambda 10^{-0.4\Delta m_\lambda}}\right) + \mathbf{P}_\lambda^{\rm sca}\frac{F_\lambda^{\rm sca}}{F_\lambda 10^{-0.4\Delta m_\lambda}}. \quad (10)$$

The term $P_\lambda^{\rm cs}$ is determined by many physical processes which are difficult to simulate. Therefore, we use the values of $P_\lambda^{\rm cs}$ and $P_\lambda^{\rm sca}$ already separated by Berdiugin *et al.* (1992) from observations of polarization of the object at different brightness levels (and from observations of nearby stars to exclude the contribution of interstellar polarization), and consider below only the $P_\lambda^{\rm sca}$ term.

Computational Methods

With the model described, we have calculated the spectral energy distribution from the visual to the far-infrared F_λ, the circumstellar extinction curves in the ultraviolet A_λ, the tracks in the color–magnitude diagrams $(U-B)$, $(B-V)$, $(V-R)$, $(V-I)$ vs ΔV, the wavelength dependence of the polarization $P_\lambda^{\rm sca}$, the intensity scans $F_\lambda(p)$, where p is the impact parameter, and the polarization maps $P_\lambda^{\rm sca}(x, y)$, where x, y are the coordinates in the plane perpendicular to the line of sight.

Polarized radiation transfer in the shell with the density distribution given by Eq. (2) was simulated with a 2D Monte Carlo

code developed by Fischer (1995). It is well known that such codes are inefficient when calculating the dust temperature T required to evaluate the term $F_\lambda^{\rm therm}$ in Eq. (3). As the optical thickness of the shells is not large it is possible to approximate the temperature profile simply as $T(\mathbf{r}) \approx T^{\rm s}(r)$, where $r = |\mathbf{r}|$ and $T^{\rm s}(r)$ is the temperature profile of the spherically symmetric shell having a power-law density distribution with the exponent α and the sizes ($R_{\rm in}$, $R_{\rm out}$) along with the mass equal to those of the shell with the density distribution given by Eq. (2).

When the temperature distribution is approximated in such a way, the infrared flux depends mainly on the radial distribution of the circumstellar dust. Therefore, the extremely time-consuming calculations with the Monte Carlo method for the shells with the spheroidal density distribution give essentially the same results as obtained in 1D modeling of the equivalent spherical shell model. Thus, to calculate the spectral energy distribution for a large number of wavelengths, we utilized the shell models with the one-dimensional density distribution described above.

The radiation transfer problem for the spherically symmetric shell models was treated with a 1D code of E. Krügel (Chini *et al.* 1986). Since this code, like most other 1D codes, operates only with sources of radiation having a blackbody spectrum, we used the following approximation to be able to compare theoretical and observed energy distributions

$$\tilde{F}_\lambda \approx F_\lambda^{\rm Kur}\left[e^{-\tau_\lambda} + \frac{F_\lambda^{\rm sca} + F_\lambda^{\rm therm}}{F_\lambda^{\rm bb}}\right], \qquad (11)$$

where $F_\lambda^{\rm Kur}$ is the flux of LTE stellar atmosphere model of Kurucz (1979), $F_\lambda^{\rm bb} = \pi B_\lambda(T_*)$, B_λ is the Planck function, and T_* is the stellar effective temperature.

Parameters of the Model

Our aim is to consider possible grain porosity effects and not to perform a detailed interpretation of observational data available for a HAeBe star. Therefore, a model of the relatively well-studied object WW Vul (spectral class A0 and distance 550 pc according to Friedemann *et al.* (1993)) which fits the observed infrared spectrum is selected, and porosity of the circumstellar grains is varied in a wide range. The values of most parameters are kept constant ($R_{\rm in} = 1.9$ AU, $R_{\rm out} = 4 \times 10^3$ AU, $\alpha = 1.5$, $A/B = 5$, $T_* = 9500$ K, $L_* = 80\,L_\odot$), and only the value of n_0 is changed along with the grain porosity so that the optical thickness of the shell in the visual $\tau_V^{\rm abs}$ (only absorption of radiation by dust) is the same.

It should be noted that there are only few main parameters of the model. For instance, in the infrared the profile of the spectral energy distribution (F_λ) is mainly dependent on the optical thickness $\tau_\lambda^{\rm abs}$ at about the wavelength of the source radiation maximum (Ivezic and Elitzur 1997, Krivova and Il'in 1997). Other important parameters are α and $R_{\rm in}$ (e.g., Krivova 1997). The remaining characteristics of the shell and of the circumstellar grain ensemble affect rather slightly the spectral energy distribution.

The tracks in the color–magnitude diagrams are mainly connected with the optical thickness $\tau_\lambda^{\rm sca}$ (only scattering of radiation by dust) in the bands of observations (see Krivova and Il'in (1997) for more details). It is a bit more difficult to find the principle parameters that determine other model characteristics such as A_λ, $P_\lambda^{\rm sh}$, and $F_\lambda(p)$ (see, e.g., Voshchinnikov *et al.* (1995, 1996), Il'in *et al.* (1996), Krivova (1998) and references therein).

3. RESULTS AND DISCUSSION

Infrared Spectra

The optical thickness of the shells in the infrared is small, and the thermal radiation of spherical (or nonspherical but not aligned) grains is isotropic. Thus, the shell orientation relative to the observer is of little significance for the total infrared flux in our model. Moreover, the flux weakly depends on the shell shape and hence on A/B (Krivova 1998). Therefore, we present and discuss the spectral energy distribution obtained for a spherically symmetric model equivalent to our spheroidal model (see Section 2 for more details).

In Fig. 1 we show the spectra calculated for the shell around WW Vul with circumstellar grains treated like those in the model of Li and Greenberg (1997). The filling factor f is in the range from 0.01 to 0.1 and the sizes of the grains are $a = 0.3$ or $0.7\ \mu$m. The effects of the porosity for Mathis (1996) and MRN grain models have been briefly discussed by Krivova *et al.* (1998) and Il'in and Krivova (2000), respectively.

As may be seen from the figure, the 10-fold decrease of the filling factor f scarcely affects the spectral energy distribution. The same result was obtained for the Mathis (1996) model with f varying from 0.45 to 0.15 (Krivova *et al.* 1998). This is not particularly surprising since the optical properties of the grains

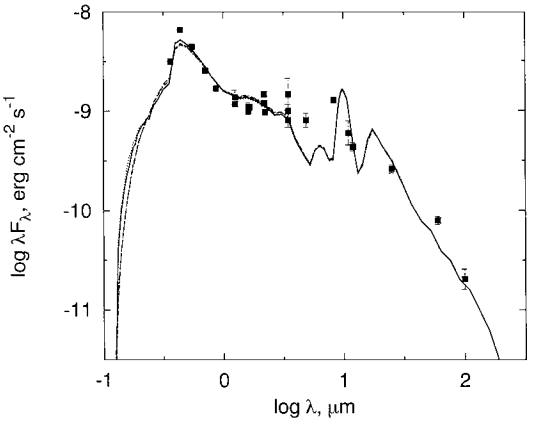

FIG. 1. Spectral energy distribution for the shell with the grains having the size $a = 0.3\ \mu$m and the filling factor $f = 0.03$ (solid line) and 0.1 (dot-dashed line), and $a = 0.7\ \mu$m and $f = 0.03$ (dashed line) and 0.01 (dotted line). The grain model of Li and Greenberg (1997) is used. The squares show observations of WW Vul by Cohen (1973), Glass and Penston (1974), Kolotilov *et al.* (1977), Weaver and Jones (1992), and Li *et al.* (1994).

regularly change with their porosity and the optical thickness $\tau_V^{\rm abs}$ was kept constant. As mentioned above, it is this parameter that primarily determines the spectral energy distribution.

A different situation arises with the MRN model, which includes two populations of grains (bare silicate and graphite particles) with quite different optical constants. The porosity of the grains affects the optical properties and hence the temperatures of silicate and graphite particles in a different way. This results in a rather complicated dependence of the spectral energy distribution on the grain fluffiness manifested mainly in the near- to mid-infrared as a change of the infrared peak shape and location and of the silicate emission bands strength (see Il'in and Krivova (2000) for more details).

As an illustration we also give in Fig. 1 the values of $F_\lambda \exp(\tau_\lambda^{\rm is})$ which are the fluxes of WW Vul observed by Cohen (1973), Glass and Penston (1974), Kolotilov *et al.* (1977), Weaver and Jones (1992), and Li *et al.* (1994) and corrected for interstellar reddening. The optical thickness $\tau_\lambda^{\rm is}$ was estimated from $E_{B-V}^{\rm is} = 0.14$ (Friedemann *et al.* 1993) in the standard way using the mean interstellar extinction curve from Whittet (1992) and the value of $R_V = A_V/E_{B-V} = 3.1$.

Note that the aim of the paper is to investigate the effects of the grain porosity on the observational manifestations of the dust shells, rather than to fit the observational data. That is why we did not look for an excellent fit to the data for WW Vul. A better agreement may be reached, for instance, by changing the optical constants of the grain materials which are not well established and should be considered rather as a parameter. On the other hand, it has been noted many times that the same spectral energy distribution can be well fitted by a rich variety of shell models (e.g., Stenholm 1990, Thamm *et al.* 1994, Men'shchikov and Henning 1996).

The flux of WW Vul at $\lambda = 1.3$ mm was measured by Natta *et al.* (1997). Even without the beam size correction (the aperture used was $11''$, which corresponds to 6000 AU for WW Vul) our theoretical point $F_\lambda \approx 0.3$ mJy is essentially below the observed value $F_\lambda \approx 10$ mJy. We do not discuss this discrepancy because in this paper we concentrate on the grains located in the inner layers of the dust shells. These are the layers which mainly contribute to the scattering and absorption of the stellar radiation in the ultraviolet and visual and to the thermal radiation in the near- and mid-infrared. Here we should only note that in the far-infrared an important role is played by the dust emissivity law $\varepsilon_\lambda \sim \lambda^\beta$ when $\lambda \to \infty$ (e.g., Harvey *et al.* 1991). The value of ε_λ is proportional to the absorption cross section $C_{\rm abs}$ averaged over the grain ensemble. The dependence of $C_{\rm abs}$ on the particle porosity was discussed many times (e.g., Ossenkopf 1991) as well as were the effects of the porosity in the infrared silicate bands at 10 and 20 μm (see, e.g., Hage and Greenberg (1990), Henning and Stognienko (1993)), and they are not considered here.

Finally, it should be mentioned that the masses of the dust shells $M_{\rm env}$ with nearly the same integrated infrared fluxes decrease with the material filling factor f for $f \lesssim 0.5$ and increase for $f \gtrsim 0.5$ (such a maximum of the opacity per mass ratio has been noted by Mathis (1996)). For WW Vul, with the grain model of Li and Greenberg (1997) we get $M_{\rm env} \approx 3.2 \times 10^{-4}\ M_\odot$ for $f = 0.1$ and $\approx 3.8 \times 10^{-4}\ M_\odot$ for $f = 0.01$.

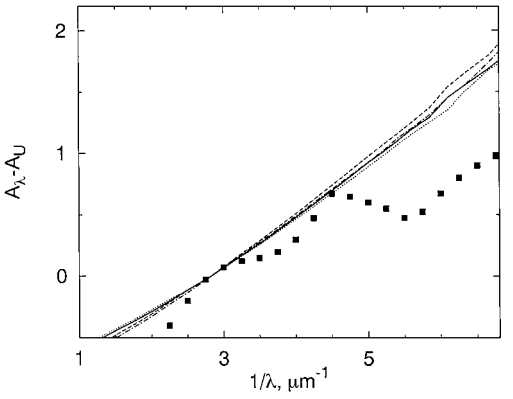

FIG. 2. The circumstellar extinction curve for the shell with the grains of different sizes and porosities. The grain parameter values and notations are as described in the legend to Fig. 1. The squares show the observations for NX Pup from Tjin A Djie *et al.* (1984).

Circumstellar Extinction Curve

The spectral energy distribution in the ultraviolet is better seen when represented in the form of a circumstellar extinction curve. In Fig. 2 we show such curves normalized to the extinction in the U band ($A_\lambda - A_U$) for the shell around WW Vul with circumstellar grains treated like those in the model of Li and Greenberg (1997). The dependence of the curves on the ratio A/B and other shell parameters may be well understood from the detailed figures given (for a bit different model) by Voshchinnikov *et al.* (1996).

The observational curve is not available for WW Vul, but it was obtained for some other HAeBe stars, e.g., HD 259431 (Sitko *et al.* 1981) and NX Pup (Tjin A Djie *et al.* 1984). In Fig. 2 we show the curve for NX Pup. This star has $T_* = 9500$ K, $L_* = 100\ L_\odot$, shows Algol-like brightness minima, and seems to be similar to WW Vul (Tjin A Djie *et al.* 1984). The circumstellar extinction curve for NX Pup is fairly similar to the curves observed for other analogous HAeBe stars (see, e.g., the curves for three HAeBe stars in Voshchinnikov *et al.* (1996)). In outline, the curves appear to show a feature at about $\lambda = 2200$ Å. It should be noted, however, that the extraction of the circumstellar extinction in the ultraviolet is a problem because of the contribution of interstellar extinction.

It is evident from Fig. 2 that both the grain porosity and size effects are rather weak. For Mathis (1996) model, the circumstellar extinction curve has also a week wavelength dependence when $f \approx 0.45$, but it becomes very steep at $1/\lambda > 5\ \mu{\rm m}^{-1}$ for $f \approx 0.15$ (Krivova *et al.* 1998). For MRN model, the curve has two features: a strong bump at $\lambda = 2200$ Åand a sharp rise at $1/\lambda > 6.5\ \mu{\rm m}^{-1}$, which essentially vary with the grain porosity (see Il'in and Krivova (2000) for more details). A cautionary note

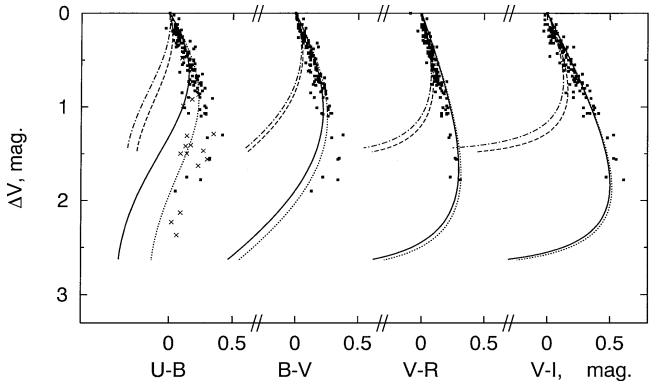

FIG. 3. The color–magnitude diagrams in the *UBVRI* bands for shells with grains of different size and porosity (the inclination angle $\varphi = 75^\circ$). Grain parameters and notations as described in the legend to Fig. 1. The observations of WW Vul by Berdiugin *et al.* (1992) are shown by squares and the data of Zaitseva (1983) by crosses.

is appropriate, however, as all these results were obtained with the EMT. This theory is known to not work well when the size of inhomogeneities of scattering particles is larger than or even comparable to the wavelength of incident radiation (e.g., Wolff *et al.* 1994, 1998; Chylek and Videen 1998; Videen and Chylek 1998) and this case may be realizable in the (far) ultraviolet.

Color–Magnitude Diagrams

Whereas the infrared spectra of the objects are mainly related to the absorption/emission properties of the circumstellar dust grains, their scattering properties may be studied by consideration of the bluing effect in the color–magnitude diagrams and of the intrinsic linear polarization. We have calculated the stellar tracks in the diagrams for WW Vul at the *UBVRI* bands. Figure 3 presents the tracks for the case of the shell having the density distribution as given by Eq. (2) and seen at the angle $\varphi = 75^\circ$.

The basic characteristics of the tracks are the maximum amplitude of the brightness decreases $(\Delta m)_{\max}$, the brightness level at which the turning points of the tracks occur $(\Delta m)_{\rm t}$, and the maximum bluing $(X-Y)_{\max}$. As mentioned by Krivova and Il'in (1997), these characteristics depend mainly on the optical thickness of the shell $\tau_\lambda^{\rm sca}$. For instance, as follows from Eq. (6) with $\tau^{\rm cl} = \infty$, the maximum brightness decrease in the visual region should be (see also Whitney *et al.* (1997))

$$(\Delta m)_{\max} = -2.5 \log \left[\frac{F_\lambda^{\rm sca}/F_\lambda^*}{e^{-\tau_\lambda} + F_\lambda^{\rm sca}/F_\lambda^*} \right] \approx -2.5 \log \tau_\lambda^{\rm sca} \big/ \left[1 - \tau_\lambda^{\rm abs}\right] \approx -2.5 \log \tau_\lambda^{\rm sca}, \quad (12)$$

where we assume that the optical thickness of the shell is small, $F_\lambda^{\rm sca}/F_\lambda^* \approx \tau_\lambda^{\rm sca}$ and $\exp(-\tau_\lambda) \approx 1 - \tau_\lambda^{\rm abs} - \tau_\lambda^{\rm sca}$.

Thus, for the stars with a low ratio of the infrared luminosity to the stellar luminosity, the value of $(\Delta m)_{\max}$ allows one to nearly directly estimate the optical thickness $\tau_\lambda^{\rm sca}$. However, one must keep in mind that the objects can have periods of increased/decreased maximum brightness and then the brightness drop must be counted from the local level of the object brightness.

For the shells under consideration, the dependence of $(\Delta m)_{\max}$ on the optical thickness is not as simple as shown above for the optically thin shells but still is quite important. As is seen from Fig. 3 for the grains of the same size ($a = 0.3\,\mu$m) but different porosity, the higher is the porosity, the larger are $(\Delta m)_{\max}$ and $(\Delta m)_{\rm t}$. As the porosity of grains P usually lowers the single-scattering albedo and the optical thickness $\tau^{\rm abs}$ is kept constant, the increase of P reduces $\tau^{\rm sca}$ and hence the fraction of scattered radiation in the visual along with the value of $(\Delta m)_{\max}$. The same is true for $(\Delta m)_{\rm t}$.

For other grain models considered, the results are similar: for more fluffy grains the turning points of the tracks occur at lower brightness levels for the same infrared fluxes.

The strength of the bluing effect (i.e., the value of $(X-Y)_{\max}$) is related, in our model, to the wavelength dependence of albedo averaged over the circumstellar grain ensemble (see Eq. (7)). It is illustrated in Fig. 3 by the curves for grains with the size $a = 0.3\,\mu$m and $f = 0.03$, and with $a = 0.7\,\mu$m and $f = 0.01$. The grains have the same albedo in the V band ($\Lambda_V = 0.24$), but the larger grains have lower albedo in the U, B bands than the smaller grains ($\Lambda_U = 0.23$ and 0.28, respectively).

The tracks are also dependent on the inclination angle φ. Because of a spherically asymmetric dust distribution and preferable scattering by the grains in forward direction, the scattered photons leave the shell in the equatorial plane more often than in the directions of the poles. A change of φ may have the effect similar to variations of the grain albedo (see Il'in and Krivova (2000) for more details). The dependence of the characteristics of the tracks on other shell parameters can be seen from the results presented in the paper of Voshchinnikov and Karjukin (1994).

In Fig. 3, we also give the observational data obtained by Berdiugin *et al.* (1992) for one minimum. They are supplemented in $(U-B)$ by the data of Zaitseva (1983) to show a deeper minimum. To fit simultaneously the observed spectral energy distribution and the color–magnitude diagrams with our shell model, one needs to have the circumstellar particles with albedo being about 0.2–0.25 in the *UBV* bands and growing with the wavelength. Note that interstellar grains appear to have albedo in these bands about 0.5–0.7 (e.g., Witt 1989).

The porosity of particles generally reduces their albedo, which solves the problem only partly as such grains have usually albedo quickly decreasing with the wavelength (see, e.g., Fig. 9 in Il'in and Krivova (2000)). Besides our porous model, in principle there could be other explanations of the observed spectral energy distribution and color–magnitude diagrams. For example, albedo of the circumstellar grains may be as high as usual (about 0.6), provided about 50% or more of the flux in the near- and mid-infrared comes from very small grains and/or large PAH molecules (see, e.g., Natta *et al.* (1993a), Natta and Krügel

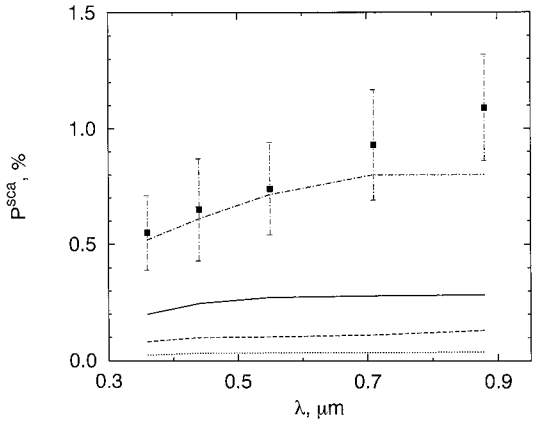

FIG. 4. The wavelength dependence of the linear polarization degree for shells with grains of different size and porosity (the inclination angle $\varphi = 75^\circ$). Grain parameters and notations as described in the legend to Fig. 1. The squares show estimates for WW Vul by Berdiugin *et al.* (1992).

1995). Another possibility is highly inhomogeneous distribution of the circumstellar dust, e.g., in the form of optically thick clumps (Friedemann *et al.* 1993, Mitskevich 1995a,b). However, we believe that these effects still need more detailed considerations.

Wavelength Dependence of Polarization

The polarization degree $P_\lambda^{\rm sca}$ calculated for grains of different porosity in the case of the Li and Greenberg (1997) model is shown in Fig. 4 for the inclination angle $\varphi = 75^\circ$ and the ratio $A/B = 5$. Note that the maximum value of $P_\lambda^{\rm sca}$ achievable when $A/B \to \infty$ is already nearly reached, as a rule, at $A/B \approx 5$ (Voshchinnikov and Karjukin (1994), Krivova (1998)). The dependence of $P_\lambda^{\rm sca}$ on the inclination angle was discussed by Il'in and Krivova (2000).

Figure 4 evidences a quick drop of $P_\lambda^{\rm sca}$ with an increase of the grain porosity. It is determined by the change of the angular dependence of intensity and polarization of radiation scattered by porous particles (see, e.g., Kozasa *et al.* (1993) for more details).

Also given in Fig. 4 are the values of $P_\lambda^{\rm sca}$ estimated by Berdiugin *et al.* (1992) from observations of WW Vul. It is clearly seen that the shell models with highly porous grains ($f \lesssim 0.01$) yield very low polarization in comparison with the observed one, and this conclusion is correct for all three grain models used.

In principle, a different geometry of the dust shells can lead to a higher degree of polarization for the same grains. The spatial dust distribution around the stars is determined by geometry and strength of magnetic fields, radiation pressure on the grains, and some other parameters. The effects of the grain porosity P on the radiation pressure force $F_{\rm pr}$ were discussed, e.g., by Mukai *et al.* (1992). Though for fluffy grains of the same volume $F_{\rm pr}$ decreases with P, the ratio of this force to gravity does not depend on P for $P \gtrsim 0.5$ and much exceeds 1 for HAeBe stars (Il'in and Krivova 2000). Therefore, when the grain motion in the shells is not controlled by the circumstellar magnetic fields (Il'in and Krivov 1994), the disk-like geometry of the shells in the form of a sphere without two polar cones (see, e.g., Men'shchikov and Henning (1997)) is most probable. For such geometry, the polarization degree $P_\lambda^{\rm sca}$ will be a bit larger than that for our spheriodal distribution, but the difference will not be as large as required to fit the observed points with very porous grains.

It should also be mentioned that to simulate the optical properties of fluffy dust grains we applied the EMT and Mie theory. Another way is to use more justified but also much more time-consuming calculations in the Discrete Dipole Approximation (DDA). A number of papers were devoted to consideration of the optical properties of dust grains within this approach (e.g., Bazell and Dwek 1990; Kozasa *et al.* 1992, 1993; Lumme and Rahola 1994, Wolff *et al.* 1994; Xing and Hanner 1997). Generally, the studies dealt with certain aspects of the problem, and a comprehensive investigation of all the effects in the case of HAeBe stars would require much more effort.

We have performed some simulations of polarized radiation transfer in the dust shells when the optical properties of the grains were calculated with the DDA. A preliminary analysis shows that the conclusions obtained with the EMT generally hold if the sizes of constituent subparticles are small ($\lesssim 0.01\ \mu$m), which could be expected, for instance, after the papers by Wolff *et al.* (1994, 1998). An increase of the subgrain sizes basically gives the same effect as a decrease of the porosity (such as lowering of albedo and growth of the polarization). The detailed results of these computations will be presented elsewhere (Krivova *et al.* 2000 in preparation).

Intensity and Polarization Maps

The shell geometry can be clarified by high angular resolution observations (see, e.g., Butner 1996, Butner *et al.* 1997). In addition, such intensity and polarization maps allow one to constrain some other shell parameters (Il'in *et al.* 1996). Then, it is also interesting to consider whether they are sensitive to the porosity of the dust grains.

We have calculated scans and intensity maps of the shells at different wavelengths. Results for the MRN model were presented by Il'in and Krivova (2000); those for other grain models look similar. As the dust temperature distribution depends scarcely on the porosity, the scans in the infrared ($\lambda = 12, 50\ \mu$m) are alike. They deviate only by a factor practically independent of the impact parameter owing to the difference between the optical thicknesses $\tau_\lambda^{\rm abs}$ (we kept $\tau_V^{\rm abs}$ constant but the wavelength dependence of $\tau_\lambda^{\rm abs}$ is dissimilar for different porosities). In the visual and near-infrared (λ 0.7, 1.65 μm), scattered light plays an important role. With a growing fluffiness of grains, the asymmetry factor $\langle \cos\theta \rangle$ also grows and more radiation is scattered in forward directions. Thus, the scattered radiation coming from the periphery layers of the shells falls off, and the scans show a steeper decline. We believe, however, that the effects of the grain porosity are not dominant in the scans. More important are the

spatial distribution of dust particles and their size and chemical composition.

It should be remarked that the intensity scans and maps have been observed for a very limited number of the brightest HAeBe stars and, with rare exception (e.g., Leinert *et al.* 1991, 1994; Marsh *et al.* 1995; Nakajima and Golimowski 1995), in the far-infrared to millimeter regions (Natta *et al.* 1993b, Di Francesco *et al.* 1997, Mannings and Sargent 1997, among others). The data available for one of the most studied objects, AB Aur, have been briefly discussed and compared with theoretical models by Il'in *et al.* (1996).

Even worse is the situation with the spatially resolved measurements of the polarization. Only few such maps have been obtained for HAeBe stars (see, e.g., Piirola *et al.* 1992, Bastien *et al.* 1994). Therefore we do not discuss them more closely. In Fig. 5 as a pattern the constructed polarization maps of the shell with grains having $f = 0.03$ and 0.01 are given for two wavelengths.

The figure evidences that besides the geometry of the shell, polarization maps are quite sensitive to the size parameter of the dust grains $x = 2\pi a/\lambda$, especially in the region where $x \approx 1$, which can be explained by the change of the asymmetry factor $\langle \cos\theta \rangle$. The porosity, however, as is seen from the plots, affects the polarization maps much less than the grain size does.

Certainly the maps in the infrared and millimeter regions can provide further important information on the grains in the periphery layers of the shells but at the moment they seem to be nothing more than an additional tool to investigate the spatial dust distribution in the shells.

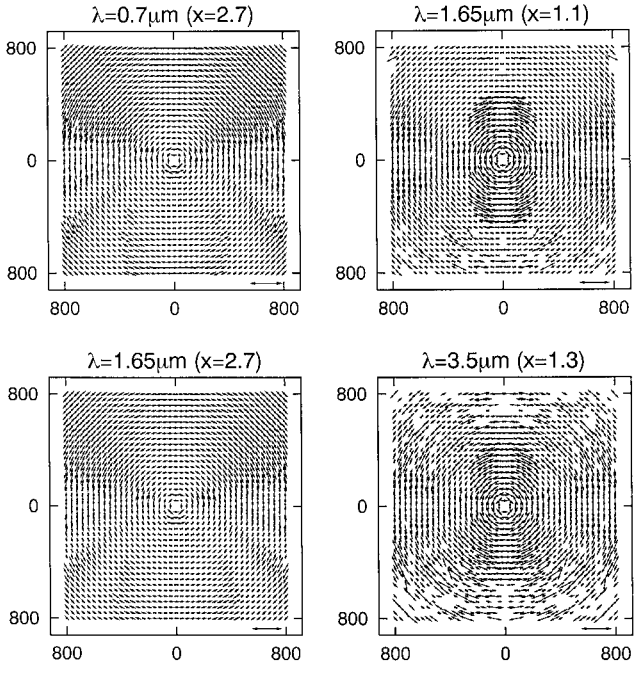

FIG. 5. Polarization maps of the central part (800 × 800 AU) of the shells with grains of the size $a = 0.3\,\mu$m and the filling factor $f = 0.03$ (top), and $a = 0.7\,\mu$m, $f = 0.01$ (bottom) at different wavelengths (indicated in each plot) for the inclination angle $\varphi = 75°$. Vectors in the right lower corners show 100% polarization.

4. CONCLUSIONS

We have performed Monte Carlo simulations of polarized radiation transfer in the dust shells of HAeBe stars, assuming a spheroidal density distribution. The circumstellar grains were represented by three fairly different grain models: (1) the model of Li and Greenberg (1997) of highly porous aggregates, (2) Mathis (1996) model of moderately porous inhomogeneous grains, and (3) the well-known MRN (Mathis *et al.* 1977) model of bare silicate and graphite grains, where we introduced fluffiness as an additional parameter. The main attention was paid to the grain porosity effects on the observational manifestations of the dust shells, such as the spectral energy distribution, the intrinsic polarization, and the peculiar behavior of color indices during brightness minima for the stars with Algol-like dimmings. In addition, intensity scans and polarization maps were also constructed for our models in view of possible future observations. We found that:

1. The porosity of grains weakly affects the profile of the spectral energy distribution when circumstellar shells do not contain particles with quite different optical properties (like bare silicate and graphite grains in the MRN model). However, the same infrared flux can be produced by different masses of porous dust: the less mass of moderately porous dust grains is required to produce the same flux as compact or, alternatively, very porous grains do.

2. As the near- and mid-infrared fluxes are mainly associated with the thermal emission of the hottest dust and the bulk of the scattered radiation comes from the most dense regions, we expect that the infrared spectra and the color–magnitude diagrams observed for HAeBe stars with Algol-like minima are attributable to the same dust grains in the innermost layers of the shells. If this is the case, then in the frame of our shell model the albedo of these grains should slightly increase with the wavelength in the visual and should be as low as about 0.2–0.3 for the grain model of Li and Greenberg (1997) (the results for other grain models are similar). The porosity of grains reduces their albedo down to the required level, although this still remains a problem with the fitting of the strength of the bluing effect seen in the color–magnitude diagrams, which stems from the change of the wavelength dependence of albedo.

3. The linear polarization of radiation of the shells drops distinctly when porosity of the grains increases. Though the flared or "fan"-shaped disk geometries could produce a noticeably higher polarization, it will hardly solve the problem in the case of highly porous (the filling factor $f \lesssim 0.03$) grains, as the polarization they produce is extremely low (this conclusion is correct for all three grain models considered).

4. The porosity of grains does not show pronounced effects in the intensity and polarization maps of the objects when compared

with the effects of the grain size or composition. On the other hand, apart from the fact that the intensity and polarization maps provide an additional tool to investigate the spatial dust distribution in the shells, they are an essential source of information about the grain properties in the outer parts of the shells, as the innermost dust will always dominate when unresolved radiation is considered (except for the far-infrared and millimeter observations).

ACKNOWLEDGMENTS

The authors are grateful to E. Krügel and O. Fischer for providing the radiative transfer codes, to H. Kimura for the DDA calculations and fruitful discussions, to A. Li for supplying us with the optical constants, to N.V. Voshchinnikov for useful comments, and in particular to the referee, A. Natta, whose remarks and suggestions essentially improved the manuscript. N.K. thanks I. Mann for offering excellent working conditions during her stay at MPAE.

The work was partly supported by a grant from the Volkswagen Foundation, Germany. V.I. acknowledges the support by the Russian Ministry of Education within the program "Universities of Russia—Fundamental Researches" (Grant N 2154).

REFERENCES

Bastien, P., F. Menard, and L. Asselin 1994. The circumstellar environment of two HAeBe stars. In *The Nature and Evolutionary Status of Herbig Ae/Be Stars* (P. S. Thé, M. R. Pérez, and E. P. J. van den Heuvel, Eds.), Astron. Soc. Pacific. Conf. Ser., Vol. 62, pp. 71–73.

Bazell, D., and E. Dwek 1990. The effects of compositional inhomogeneities and fractal dimension on the optical properties of astrophysical dust. *Astrophys. J.* **360**, 142–150.

Berdiugin, A. V., V. P. Grinin, and N. H. Minikulov 1992. The optical dichroism of the circumstellar dust and intrinsic polarization of WW Vul. *Izv. Krym. Astrofiz. Obs.* **86**, 69–96.

Berrilli, F., G. Corciulo, G. Ingrosso, D. Lorenzetti, B. Nisini, and F. Strafella 1992. Infrared emission from dust structures surrounding Herbig Ae/Be stars. *Astrophys. J.* **398**, 254–272.

Bohren, C. F., and D. R. Huffman 1983. *Absorption and Scattering of Light by Small Particles*. Wiley, New York.

Butner, H. 1996. Far-infrared spatial observations of Herbig Ae/Be stars and low mass stars. In *The Role of Dust in the Formation of Stars* (H. U. Käufl and R. Siebenmorgen, Eds.), pp. 149–156. Springer-Verlag, Berlin/New York.

Butner, H. M., G. H. Moriarty-Schieven, P. G. Wannier, M. W. Werner, M. E. Ressler, R. Evans, and D. A. Harper 1997. Probing the envelopes of young stellar objects through far-infrared mapping. *Bull. Am. Astron. Soc.* **190**, 4116.

Chini, R., E. Krügel, and E. Kreysa 1986. Dust emission spectra from star-forming regions. *Astron. Astrophys.* **167**, 315–324.

Chylek, P., and G. Videen 1998. Scattering by a composite sphere and effective medium approximations. *Opt. Commun.* **146**, 15–20.

Cohen, M. 1973. Infra-red observations of young stars—II. T Tauri stars and the Orion Population. *Mon. Not. R. Astron. Soc.* **161**, 97–104.

Di Francesco, J., N. J. Evans II, P. M. Harvey, L. G. Mundy, S. Guilloteau, and C. J. Chandler 1997. Millimeter and radio interferometry of Herbig Ae/Be stars. *Astrophys. J.* **482**, 433–441.

Draine, B. T. 1994. Dust in diffuse interstellar clouds. In *The Infrared Cirrus and Diffuse Interstellar Clouds*. (R. M. Cutri and W. B. Latter, Eds.), Astron. Soc. Pacific. Conf. Ser., Vol. 58, pp. 227–243.

Fischer, O. 1995. Polarization by interstellar dust—Modelling and interpretation of polarization maps. *Rev. Mod. Astron.* **8**, 103–124.

Friedemann, C., H. G. Reimann, J. Gürtler, and V. Tóth 1993. The cloudy circumstellar dust shell of WW-Vulpeculae revisited. *Astron. Astrophys.* **277**, 184–194.

Glass, I., and M. Penston 1974. An infrared survey of RW Aurigae stars. *Mon. Not. R. Astron. Soc.* **167**, 237–249.

Greenberg, J. M., and J. I. Hage 1990. From interstellar dust to comets: A unification of observational constraints. *Astrophys. J.* **361**, 260–274.

Grinin, V. P. 1988. On the blue emission visible during deep minima of young irregular variables. *Astron. Lett.* **14**, 27–28.

Grinin, V. P. 1994. Polarimetric activity of Herbig Ae/Be stars. In *The Nature and Evolutionary Status of Herbig Ae/Be Stars* (P. S. Thé, M. R. Pérez, and E. P. J. van den Heuvel, Eds.), Astron. Soc. Pacific. Conf. Ser., Vol. 62, pp. 63–70.

Grinin, V. P., N. N. Kiselev, G. P. Chernova, N. K. Minikulov, and N. V. Voshchinnikov 1991. The investigations of 'zodiacal light' of isolated Ae-Herbig stars with nonperiodic Algol-type minima. *Astrophys. Space Sci.* **186**, 283–298.

Grinin, V. P., A. Natta, and L. Tambovtseva 1996. Evaporation of star-gazing bodies in the vicinity of UX Orionis-type stars. *Astron. Astrophys.* **313**, 857–865.

Hage, J. I., and J. M. Greenberg 1990. A model for the optical properties of porous grains. *Astrophys. J.* **361**, 251–259.

Harper, D. A., R. F. Loewenstein, J. A., and Davidson 1984. On the nature of the material surrounding Vega. *Astrophys. J.* **285**, 808–812.

Harvey, P. M., D. F. Lester, D. Brock, and M. Joy 1991. Dust properties around evolved stars from far-infrared size limits. *Astrophys. J.* **368**, 558–563.

Henning, Th. 1997. Interstellar dust grains—An overview. In *Molecules in Astrophysics: Probes and Processes* (E. F. van Dishoek, Ed.), pp. 343–356. Kluwer, Dordrecht.

Henning, Th., and R. Stognienko 1993. Porous grains and polarization of light: The silicate features. *Astron. Astrophys.* **280**, 609–616.

Herbst, W., D. K. Herbst, and E. J., Grossman 1994. Catalogue of UBVRI photometry of T Tauri stars and analysis of the causes of their variability. *Astron. J.* **108**, 1906–1923.

Il'in, V. B., and A. V. Krivov 1994. Dynamics of small grains near Herbig Ae stars. In *The Nature and Evolutionary Status of Herbig Ae/Be Stars* (P. S. Thé, M. R. Pérez, and E. P. J. van den Heuvel, Eds.), Astron. Soc. Pacific. Conf. Ser., Vol. 62, pp. 177–180.

Il'in, V. B., and N. A. Krivova 2000. On fluffiness of grains in the shells of Herbig Ae/Be stars. *Astron. Lett.*, in press.

Il'in, V., N. Krivova, and A. Men'shchikov 1996. Modelling of the IR intensity maps for HAEBE stars with Algol-like minima. In *The Role of Dust in the Formation of Stars* (H. U. Käufl and R. Siebenmorgen, Eds.), pp. 183–186. Springer-Verlag, Berlin/New York.

Ivezic, Z., and M. Elitzur 1997. Self-similarity and scaling behavior of infrared emission from radiatively heated dust—I. Theory. *Mon. Not. R. Astron. Soc.* **287**, 799–811.

Kolotilov, Ye. A., G. V. Zaitseva, and V. I. Shenavrin 1977. Spectral and photometric observations of fast irregular variables. III. VX Cas, UX Ori, BN Ori and WW Vul. Results of U, B, V, J, H, K, L photometry. *Astrofiz.* **13**, 253–260.

Kozasa, T., J. Blum, and T. Mukai 1992. Optical properties of dust aggregates. I—Wavelength dependence. *Astron. Astrophys.* **263**, 423–432.

Kozasa, T., J. Blum, H. Okamoto, and T. Mukai 1993. Optical properties of dust aggregates. II. Angular dependence of scattered light. *Astron. Astrophys.* **276**, 278–288.

Krivova, N. A. 1997. Herbig Ae stars with Algol-like minima: Modeling of the spectral energy distribution and of the behavior of colors at minima. *Astron. Lett*. **23**, 327–337.

Krivova, N. A. 1998. *Dust Shells of UX Ori-type Stars: Modelling and Interpretation of Observational Data*. Ph.D. thesis, St. Petersburg State University, St. Petersburg.

Krivova, N. A., and V. B. Il'in 1997. Dust shells around Herbig Ae/Be stars with Algol-like minima: Modeling of photometric observations. *Astron. Lett*. **23**, 791–798.

Krivova, N. A., V. B. Il'in, and H. Kimura 1998. Dust around Herbig Ae/Be stars: Modelling of observational data. *Earth Planets Space* **50**, 603–606.

Kurucz, R. L. 1979. Model atmospheres for G, F, A, B, and O stars. *Astrophys. J. Suppl. Ser*. **40**, 1–340.

Laor, A., and B. T. Draine 1993. Spectroscopic constraints on the properties of dust in active galactic nuclei. *Astrophys. J*. **402**, 441–468.

Leinert, C., M. Haas, and R. Lenzen 1991. LkHα 198 and V 376 Cassiopeiae—Speckle interferometric and polarimetric observations of circumstellar dust. *Astron. Astrophys*. **246**, 180–194.

Leinert, C., A. Richichi, N. Weitzel, and M. Haas 1994. Near-infrared speckle observations of Herbig Ae/Be stars. In *The Nature and Evolutionary Status of Herbig Ae/Be Stars* (P. S. Thé, M. R. Pérez, and E. P. J. van den Heuvel, Eds.), Astron. Soc. Pacific. Conf. Ser., Vol. 62. pp. 155–166.

Li, A., and J. M. Greenberg 1997. A unified model of interstellar dust. *Astron. Astrophys*. **323**, 566–584.

Li, A., and J. M. Greenberg 1998. A comet dust model for the β Pictoris disk. *Astron. Astrophys*. **331**, 291–313.

Li, W., N. J. Evans II, P. M. Harvey, and C. Colome 1994. Near-infrared (J, H, K) imaging of Herbig Ae/Be stars. *Astrophys. J*. **433**, 199–215.

Lumme, K., and J. Rahola 1994. Light scattering by porous dust particles in the discrete-dipole approximation. *Astrophys. J*. **425**, 653–667.

Mannings, V., and A. I. Sargent 1997. A high-resolution study of gas and dust around young intermediate-mass stars: Evidence for circumstellar disks in Herbig Ae systems. *Astrophys. J*. **490**, 792–802.

Marsh, K. A., J. E. Van Cleve, M. J. Mahoney, T. L. Hayward, and J. R. Houck 1995. Spatially resolved mid-infrared observations of circumstellar dust around AB Aurigae. *Astrophys. J*. **451**, 777–783.

Mathis, J. S. 1990. Intestellar dust and extinction. *Annu. Rev. Astron. Astrophys*. **28**, 37–70.

Mathis, J. S. 1996. Dust models with tight abundance constraints. *Astrophys. J*. **472**, 643–655.

Mathis, J. S. 1998. The near-infrared intestellar silicate bands and grain theories. *Astrophys. J*. **497**, 824–832.

Mathis, J. S., W. Rumpl, and K. H. Nordsieck 1977. The size distribution of interstellar grains. *Astrophys. J*. **217**, 425–433.

Men'shchikov, A. B., and Th. Henning 1996. 2d radiative transfer models of the embedded YSOs HL Tau and L1551 IRS 5: What is inside. In *The Role of Dust in the Formation of Stars* (H. U. Käufl and R. Siebenmorgen, Eds.), pp. 351–354. Springer-Verlag, Berlin/New York.

Men'shchikov, A. B., and Th. Henning 1997. Radiation transfer in circumstellar disks. *Astron. Astrophys*. **318**, 879–907.

Miroshnichenko, A., Z. Ivezic, and M. Elitzur 1997. On protostellar disks in Herbig Ae/Be stars. *Astrophys. J*. **475**, L41–L44.

Mitskevich, A. 1995a. Circumstellar environment, infrared excess and variable extinction in young stars. I. The model. *Astron. Astrophys*. **298**, 219–230.

Mitskevich, A. 1995b. Circumstellar environment, infrared excess and variable extinction in young stars. II. Discussion. *Astron. Astrophys*. **298**, 231–242.

Mukai, T., H. Ishimoto, T. Kozasa, J. Blum, and J. M. Greenberg 1992. Radiation pressure forces of fluffy porous grains. *Astron. Astrophys*. **262**, 315–320.

Nakajima, T., and D. A. Golimowski 1995. Coronagraphic imaging of pre-main-sequence stars: Remnant envelopes of star formation seen in reflection. *Astron. J*. **109**, 1181–1198.

Natta, A., and E. Krügel 1995. PAH emission from Herbig Ae/Be and T Tauri stars. *Astron. Astrophys*. **302**, 849–860.

Natta, A., V. P. Grinin, V. Mannings, and H. Ungerechts 1997. The evolutionary status of UX Orionis-type stars. *Astrophys. J*. **491**, 885–890.

Natta, A., F. Palla, H. Butner, N. J. Evans II, and P. Harvey 1993a. Infrared studies of circumstellar matter around Herbig Ae/Be and related stars. *Astrophys. J*. **406**, 674–691.

Natta, A., T. Prusti, and E. Krügel 1993b. Very small dust grains in the circumstellar environment of Herbig Ae/Be stars. *Astron. Astrophys*. **275**, 527–533.

Ossenkopf, V. 1991. Effective-medium theories for cosmic dust grains. *Astron. Astrophys*. **251**, 210–219.

Pezzuto, S., F. Strafella, and D. Lorenzetti 1997. On the circumstellar matter distribution around Herbig Ae/Be stars. *Astrophys. J*. **485**, 290–307.

Piirola, V., F. Scaltriti, and G. V. Coyne 1992. Circumstellar disks deduced from subarcsecond polarization observations of two young stars. *Nature* **359**, 399–401.

Rouleau, F., and P. G. Martin 1991. Shape and clustering effects on the optical properties of amorphous carbon. *Astrophys. J*. **377**, 526–540.

Sitko, M., B. Savage, and M. Meade 1981. Ultraviolet observations of hot stars with circumstellar dust shells. *Astrophys. J*. **246**, 161–183.

Sorrell, W. H. 1990. Constraints on astronomical silicate dust. *Astrophys. J*. **361**, 150–154.

Stenholm, L. G. 1990. Molecular cloud fluctuations. II—Methods of analysis of cloud maps. *Astron. Astrophys*. **232**, 495–509.

Stognienko, R., Th. Henning, and V. Ossenkopf 1995. Optical properties of coagulated particles. *Astron. Astrophys*. **296**, 797–809.

Telesco, C. M., R. Decher, E. E. Becklin, and R. D. Wolstencroft 1988. Resolution of the circumstellar disk of Beta Pictoris at 10 and 20 microns. *Nature* **335**, 51–53.

Thamm, E., J. Steinacker, and Th. Henning 1994. Ambiguities of parameterized dust disk models for young stellar objects. *Astron. Astrophys*. **287**, 493–502.

Thé, P. S., D. De Winter, and M. R. Pérez 1994. A new catalogue of members and candidate members of the Herbig Ae/Be (HAEBE) stellar group. *Astron. Astrophys. Suppl. Ser*. **104**, 315–339.

Tjin A Djie, H. R. E., L. Remijn, and P. S. Thé 1984. A study of the Herbig Ae-type stars UX Ori and CD-44°3318 based on IUE spectra, and on visual and infrared photometry. *Astron. Astrophys*. **134**, 273–283.

Videen, G., and P. Chylek 1998. Scattering by a composite sphere with an absorbing inclusion and effective medium approximations. *Opt. Commun*. **158**, 1–6.

Voshchinnikov, N. V. 1989. Dust around young stars. Model of the Algol-type minima for UX Orionis-type stars. *Astrofiz*. **30**, 312–321.

Voshchinnikov, N. V., and V. P. Grinin 1991. Dust around young stars—Model of envelope of the Ae Herbig star WW-Vulpeculae. *Astrofiz*. **34**, 84–95.

Voshchinnikov, N. V., and V. V. Karjukin 1994. Multiple scattering of polarized radiation in circumstellar dust shells. *Astron. Astrophys*. **288**, 883–896.

Voshchinnikov, N. V., V. P. Grinin, and V. V. Karjukin 1995. Monte Carlo simulation of light scattering in the envelopes of young stars. *Astron. Astrophys*. **294**, 547–554.

Voshchinnikov, N. V., F. J. Molster, and P. S. Thé 1996. Circumstellar extinction of pre-main-sequence stars. *Astron. Astrophys*. **312**, 243–255.

Weaver, W. B., and G. Jones 1992. A catalog of co-added IRAS fluxes of Orion population stars. *Astrophys. J. Suppl. Ser*. **78**, 239–266.

Weissman, P. R. 1985. The origin of comets—Implications for planetary formation. In *Protostars and Planets II* (D. C. Black and M. S. Matthews, Eds.), pp. 895–919. Univ. of Arizona Press, Tucson.

Whitney, B. A., S. J. Kenyon, and M. Gomez 1997. Near-infrared imaging polarimetry of embedded young stars in the Taurus-Auriga molecular cloud. *Astrophys. J.* **485**, 703–718.

Whittet, D. C. B. 1992. *Dust in the Galactic Environment*. The Graduate Series in Astronomy, Institute of Physics Publishing, Bristol, UK.

Witt, A. N. 1989. Visible/UV scattering by interstellar dust. In *Interstellar Dust* (L. J. Allamandola and A. G. G. M. Tielens, Eds.), IAU Symp. 135, p. 87. Reidel, Dordrecht.

Wolff, M. J., G. C. Clayton, and S. J. Gibson 1998. Modeling composite and flufly grains. II. Porosity and phase functions. *Astrophys. J.* **503**, 815–830.

Wolff, M. J., G. C. Clayton, P. G. Martin, and R. E. Schulte-Ladbeck 1994. Modeling composite and fluffy grains: The effects of porosity. *Astrophys. J.* **423**, 412–425.

Xing, Z., and M. Hanner 1997. Light scattering by aggregate particles. *Astron. Astrophys.* **324**, 805–820.

Zaitseva, G. 1983. The photoelectric photometry of WW-Vulpeculae in 1967–1982. *Perem. Zvezdy* **22**, 1.

Zaitseva, G. V., and V. M. Lyutyi 1997. On the origin of optical variability of WW Vulpeculae. *Astron. Lett.* **23**, 242–256.